Article

Research on milling tool wears Prediction based on 3-D finite element process simulation

Zhibo LIU [1] , Caixu YUE [1], Xiaochen LI [1], Xianli LIU [1],Steven Y. Liang[2], Lihui Wang [3]

(1. The lab of National and Local United Engineering for High-Efficiency Cutting & Tools, Harbin University of Science and Technology, Harbin 150080；
2. George W. Woodruff School of Mechanical Engineering, Georgia Institute of Technology, Atlanta, USA；
3. KTH Royal Institute of Technology, Stockholm, Sweden)

[1] Zhibo LIU; simplelzb@163. com
[2] Caixu YUE; yuecaixu@hrbust. edu. cn
[3] Xiaochen LI; 18845156457@163. com
[4] Xianli LIU; xlliu@hrbust. edu. cn
[5] Steven Y. Liang; steven. liang@me. gatech. edu
[6] Lihui Wang; lihui. wang@iip. kth. se
* Correspondence: yuecaixu@hrbust. edu. cn; Tel. : +86 18846939745

Abstract: In the process of metal cutting, the anti-wear performance of the tool determines the life of the tool and affects the surface quality of the workpiece. The finite element simulation method can directly show the tool wear state and morphology, but due to the limitations of the simulation time and complex boundary conditions, it has not been commonly used in tool life prediction. Based on this, a tool wear model was established on the platform of a finite element simulation software for the cutting process of titanium alloy TC4 by end milling. The key technique is to embed different types of tool wear models into the finite element model in combination with the consequent development technology. The effectiveness of the tool wear model is validated by comparing the experimental results with the simulation results. At the same time, in order to quickly predict the tool life, an empirical prediction formula of tool wear was established, and the change course of tool wear under time change was obtained.

Keywords: Milling；Finite element simulation；Tool wear；Tool life prediction

1. Introduction

With the development of manufacturing industry, the surface performance of parts is more and more demanding. Tool wear directly affects the workpiece processing quality, tool life and processing cost, and has accurate time-varying characteristics, so many scholars have carried out research on tool wear. Scholars mostly use experimental method or analytic method to predicted tool wear, but few people adopt the method of finite element simulation to study tool wear, the main reason is that tool wear is a complicated process. Finite element simulation that carried out from the engineering direction must neglected many factor ,which also caused many limitations included a long simulation and complex boundary conditions and so on. With the improvement of computer hardware calculation speed and software simulation efficiency, the finite element simulation method can effectively simulate the course of tool wear by considering the characteristics of milling process such as depth of cut variation.

In the research on tool abrasion simulation in analytic method, scholars find the tool abrasion is influenced by the cutting parameter, geometrical parameter of tool, cutting edge form of tool, cooling method, lubrication method, etc. and make the relevant research. In order to reveal the influence of cutting parameter on tool abrasion, S. K. Choudhury et al. [1] first established the analytic model of tool abrasion for the lathe tool without coating and researched the influence of feed rate and main

Preprints (www.preprints.org) | NOT PEER-REVIEWED | Posted: 4 November 2020 doi:10.20944/preprints202011.0189.v1

shaft's rotating speed on tool abrasion. J. M. Zhou at al. [2] calculated the stress distribution of tool nose in finite element method and finally worked out the optimal tool chamfering parameter. With regard to the influence of tool's geometrical shape on tool abrasion, B. Denkena et al. [3]got the service life graph of lathe tools with different cutting edges microstructure in experiment research method, and later Rathod et al. [4]established prediction model of abrasion of lathe tool's flank surface by considering the influence of rake angle and clearance angle on abrasion of lathe tool's flank surface. Further, H. Z. Liu et al. [5]established the geometric model in which the rake angle, clearance angle and cutting edge radius were comprehensively considered, defined evaluation index of tool abrasion loss - tool abrasion volume fraction, and found the abrasion was closely related to rake angle, but unrelated to the radius of cutting edge through experiment. The cutting force and cutting temperature are key factors. G. C. Zhang et al. [6], based on the energy consumption method, established the abrasion model of flank surface to research the influence of cutting force on tool abrasion. The contact status between tool cuttings or tool technique also influences tool abrasion. Salman Pervaiz et al. [7], in the cutting process, cooled cutting process with the mixture of air and vegetable oil, and found that tool abrasion speed declined obviously. And PC Wanigarathne et al. [8]researched the influence of temperature on tool abrasion through experiment, and established the coupling relationship between cutting temperature and cutting force in cutting process.

With regard to the complex cutting process, the finite element simulation method is adopted to see the tool abrasion shape and abrasion depth intuitively. In the research on simulation of tool abrasion in finite element method, most scholars obtain abrasion results by compiling subprogram. A. Attanasio, E. Ceretti et al. [9]carried out the finite element simulation analysis to the tool abrasion in processing process through DEFORM software, and proposed different abrasion calculation models on account of tool abrasion at different temperatures. As a result, the research results improved the simulation precision. M. Binder, F. Klocke et al. [10], based on the abrasion calculation through DEFORM software, carried out the finite element simulation to the tool with different coating, and expanded the application of finite element in mechanical processing field by considering the element inversion, etc. in abrasion process. Further, Mohammad Lotfi et al. [11], based on the secondary development of deform software, proposed three-dimensional finite element simulation method of tool abrasion with ultrasound-assisted rotary turning, and researched the influence of vibration and rotational motion on tool abrasion and heating. As a result, the surface quality and cutting force improved greatly, compared with that of conventional turning. F. Faini et al. [12]researched the tool abrasion in drilling process, and got the abrasion appearance of bore bit after drilling and the tool abrasion loss after the secondary development of DEFORM software. Xie Lijing et al. [13] utilized the secondary development technology of ABAQUS to research the tool abrasion due to turning processing or Polygon cutting, and proposed the prediction method of tool abrasion based on ABAQUS software. Sun Yujing et al. [14]got the tool abrasion loss in two-dimensional milling process through The Third Wave of finite element simulation software, and embedded diffusion model in finite element simulation to verify the accuracy of model. Amir Malakizadi et al. [15]also proposed a kind of modeling method of three-dimensional tool abrasion finite element. The difference was that the calculation efficiency of abrasion model improved greatly. Such vale was calculated through an independent MATLAB code, instead of iteration, to shorten simulation time and improve simulation efficiency.

To sum up, current research focuses on predicting tool abrasion in metal cutting by empirical modeling and physics-based modeling. There are few researches on predicting tool abrasion course and tool service life in the finite element method, and the analytical method doesn't display the tool abrasion intuitively. Scholars center on predicting specific abrasion loss, and there are less researches on the tool abrasion position and the prediction method of wear appearance. Based on the existing cutting finite element simulation and theoretical model of tool abrasion, the abrasion of flank surface on end mill is simulated in finite element method for the milling process of titanium alloy Ti6Al4V. In the meantime, the simulation results are put in empirical formula to predict the service life of tool, and the milling practice is adapted to predict the precision of model.

2. Compilation of subprogram and establishment of milling finite element simulation model

Preprints (www.preprints.org) | NOT PEER-REVIEWED | Posted: 4 November 2020 doi:10.20944/preprints202011.0189.v1

2. 1. Design of subprogram for the tool abrasion prediction

The computation program flow of tool abrasion course is shown in Fig. 1. In order to accelerate simulation speed and improve simulation efficiency, the traditional iterative algorithm isn't adopted. The subprogram of users will become a part of finite element simulation, through which the value of node stress and node temperature is withdrawn from simulation results and calculated to work out the abrasion loss of cutting edge. Wear model actually takes temperature and stress as inputs. The node coordinates are updated based on the abrasion loss after calculation to update the geometrical shape of tool and reach abrasion status. Later, the abrasion value is put in empirical formula to calculate the tool abrasion course and complete predicting service life of tool. In the finite element simulation model with three-dimensional cutting, since the tool abrasion loss is far less than the element dimension, the node displacement is adopted to reach the tool abrasion effect, without considering the element deletion of tool cutting edge incurred due to abrasion in this research, in order to improve the simulation speed and adapt to the application of this engineering.

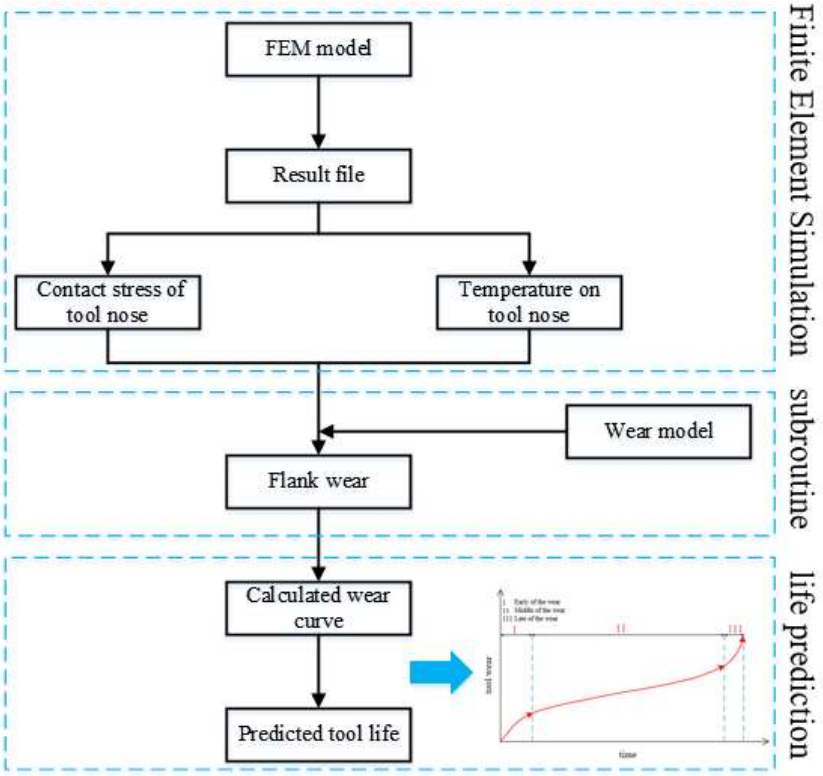

Fig. 1 Flow Chart of Abrasion Simulation

2. 2. Establishment of milling simulation model

2. 2. 1. Ti6Al4V constitutive model

The constitutive model[16]of Johnson-Cook is adopted to describe the material flow stress of work piece, and such model expresses equivalent stress, equivalent plastic strain, equivalent plastic strain rate and temperature, with the model expression formula shown in Fig. 1:

$$\bar{\sigma} = \left[A + B(\bar{\varepsilon})^n\right]\left[1 + C\ln\left(\frac{\dot{\bar{\varepsilon}}}{\dot{\bar{\varepsilon}}_o}\right)\right]\left[1 - \left(\frac{T - T_r}{T_m - T_r}\right)^m\right] \quad (1)$$

Wherein: $\bar{\sigma}$、$\bar{\varepsilon}$、$\dot{\bar{\varepsilon}}$、$\dot{\bar{\varepsilon}}_0$ represent the equivalent flow stress, equivalent plastic strain, equivalent plastic strain rate and reference strain rate; A, B, n, C and m, as material constants, represent the yield strength, strain strengthening coefficient, strain hardening parameter, strain rate sensitivity coefficient and thermal softening coefficient in quasi-static condition, respectively, which can be

Preprints (www.preprints.org) | NOT PEER-REVIEWED | Posted: 4 November 2020 doi:10.20944/preprints202011.0189.v1

calculated through tensile compression test of materials; T_r represents room temperature, at 25℃ in general; T_m represents melting temperature of materials. The material parameter of Ti6Al4V adopted in this paper is gotten through the Hopkinson pressure lever experiment, with the specific parameters as shown in Table 1].

Table 1 Johnson-cook constitutive parameter of Ti6Al4V [16]

Material	*A*/MPa	*B*/MPa	*C*	*n*	*m*
T6Al4V	543. 75	1363. 6	0. 127	0. 33	0. 303

2. 2. 2. Friction model

In the cutting process, the rack face and flank surface of the tool have friction with cuttings and work piece, respectively, the friction coefficient is related to the cutting temperature, cuttings sliding speed and normal stress of surface, and the friction size and distribution features influence the cutting temperature, cutting stress, tool abrasion, surface integrity, etc. In order to embed the compound abrasion model in simulation model, the coefficient of local friction is needed at the contact part between tool and work piece. Currently, the friction model proposed by Wang Xiaoqin[17]is adopted to describe the relationship between temperature and friction coefficient in the cutting process. Friction model is shown in Formula 2:

$$u(T) = 0.41 - \frac{0.103(T-25)}{1000} \tag{2}$$

Wherein: The u represents the friction coefficient, T represents the temperature (unit: °C). The formula (2) shows the friction coefficient decreases with the increase of temperature. Fig. 2(a) shows the stress distribution curve on contact surface of cuttings in the temperature-related friction model, in which the normal stress changes constantly and continuously with different contact points of cuttings, reaches the maximum value at tool nose, then gradually decreases and reaches 0 at the tool-cuttings separation position. Fig. 2(b)[17]shows the approximation relation existing between the friction coefficient and friction temperature as shown in formula 2, in which the friction coefficient can be deemed as the temperature-related function.

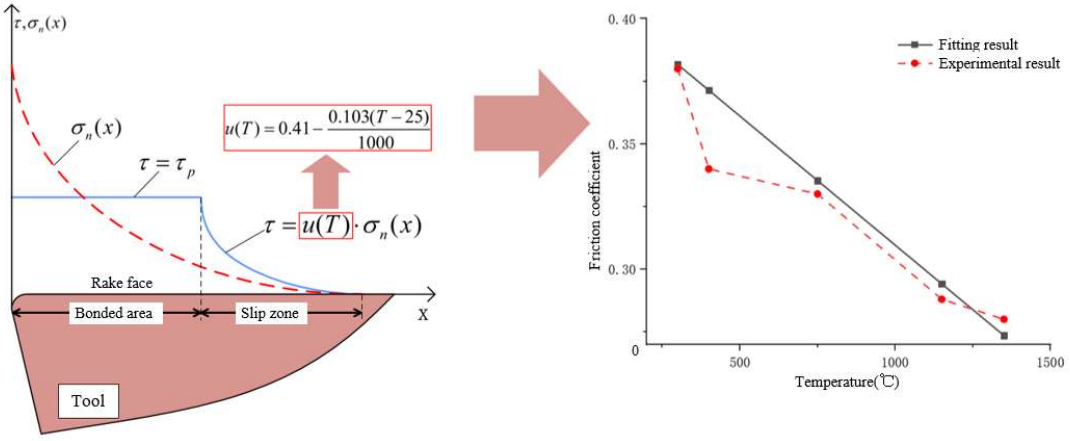

(a) (b)

Fig. 2 Temperature-related Friction Model ; (a) Stress distribution of tool-cuttings contact surface (b) Relationship between friction coefficient and temperature

2. 2. 3. Damage model

The Johnson-Cook damage model proposed by G. R. Johnson et al. is adopted in this paper and can accurately reflect the failure mechanism of common metal materials. The model formula is shown in formula (3)[16]:

Preprints (www.preprints.org) | NOT PEER-REVIEWED | Posted: 4 November 2020 doi:10.20944/preprints202011.0189.v1

$$\omega=\sum_{j=1}^{n}\left(\frac{\overline{\Delta\varepsilon^{pl}}}{\overline{\varepsilon_D^{pl}}}\right) \tag{3}$$

Wherein: $\Delta\varepsilon^{\overline{pl}}$ represents the equivalent plastic strain increments; $\varepsilon_D^{\overline{pl}}$ represents the failure strain.

If the materials in formula (1) have failure behaviors, $\omega>1$ $\varepsilon_D^{\overline{pl}}$ the failure strain formula is shown in formula (4) [16]:

$$\varepsilon_D^{\overline{pl}}=\left[d_1+d_2\exp(d_3\frac{\sigma_p}{\sigma_{\min}})\right]\left[1+d_4\ln\left(\frac{\dot{\overline{\varepsilon}}}{\dot{\overline{\varepsilon}}_0}\right)\right]\left[1+d_5\left(\frac{T-T_{\text{room}}}{T_{\text{melt}}-T_{\text{room}}}\right)\right] \tag{4}$$

Wherein: $\dot{\overline{\varepsilon}}_0$ represents the reference strain rate; $\dot{\overline{\varepsilon}}$ represents the plastic strain rate; *d_1, d_2, d_3, d_4 and d_5 represents the failure parameters of materials.*

Failure parameter value of titanium alloy TC4 researched in this paper is shown in Table 2:

Tab. 2 Johnson-cook failure parameter of TC4[16]

d1	*d2*	*d3*	*d4*	*d5*
-0. 09	0. 25	-0. 5	0. 014	3. 87

2. 2. 3. Cuttings separation criterion

Metal cutting process is accompanied by deformation and separation of materials, so the reasonable separation criterion of cuttings is needed to accurately reflect the mechanical property and physical property of work piece material. Cuttings separation criterion adopted in this paper regards energy as cuttings separation standards, with mathematical model shown in formula (5)[16]:

$$\begin{cases} D=\dfrac{\int_0^u \overline{\sigma}\,\mathrm{d}\,\overline{u^{pl}}}{G_f} \\ G_f=\dfrac{1-v^2}{E}K^2 \end{cases} \tag{5}$$

Wherein: $\overline{u^{pl}}$ represents the equivalent plastic displacement; D represents the failure displacement; G_f represents the fracture energy; K represents the fracture toughness of materials, and the final failure displacement is calculated as 0. 005mm.

2. 3. Grid partition of finite element model

Macroscopically, milling processing is an intermittent cutting process, and the action point of cutting force changes constantly. Microscopically, the milling can be simplified as orthogonal cutting or bevel cutting. In the finite element simulation, the cutting process is simulated mainly through the element failure occurred upon the contact between tool and work piece element.

In the plastic deformation containing thermal coupling simulation, the ABAQUS/Explicit module is usually adopted for analysis, and the dimension and type of grid is directly related to the precision of simulation results. In the three-dimensional plane of pre-processing with work piece dimension of 60mm*40mm*40mm, the work piece adopts CPE4RT grid and contains 800,000 regular tetrahedron element. The insulation lasts for about 15-20 hours, and the established finite element model is shown in Fig. 3. The tool adopts the overall end mill with rake angle, clearance angle and helical angle of 8°, 9° and 55°, respectively, and the blunt diameter of cutting edge of 0. 015mm. Milling processing parameters are as follows: cutting depth: 6mm, cutting width: 3 mm, feed speed: 400mm/min and rotating speed of tool: 2000r/min. Geometric model of tool after completion of NX9. 0 is led to finite element software ABAQUS in step format.

Preprints (www.preprints.org) | NOT PEER-REVIEWED | Posted: 4 November 2020 doi:10.20944/preprints202011.0189.v1

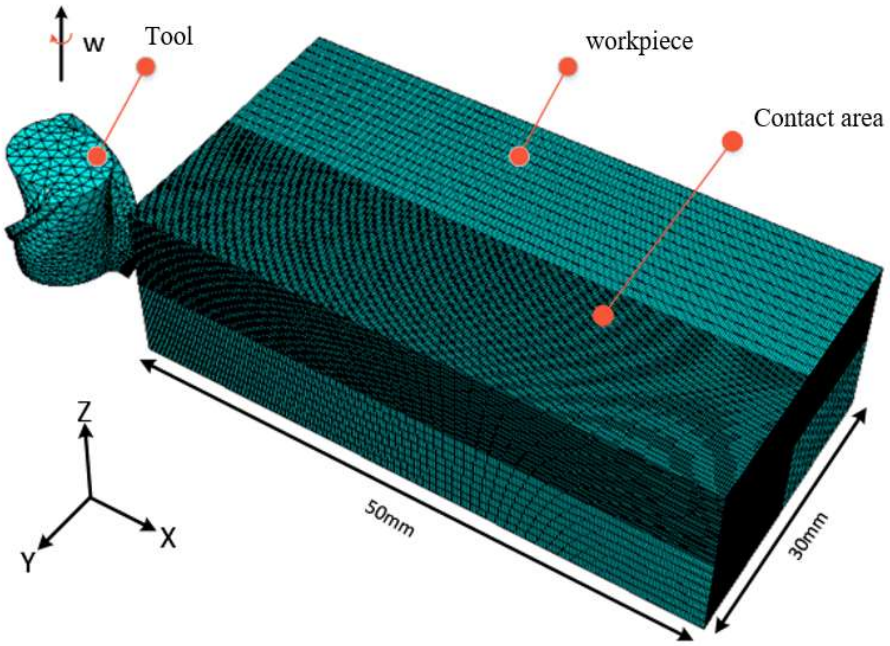

Fig. 3 Finite Element Simulation Model

In the pre-processing, tool adopts the wedge-shaped grid. The tool grid shall be moderate in the size because the over-sized grid would influence the value simulation precision and under-sized grid would generate negative volume in update process of grid, as shown in Fig. 4. If there is larger displacement at the cutting edge node, the nodes on surface would move to other elements which generate negative volume. The large grid would influence simulation precision. So the grid shall adopt the wedge-shaped element with side length of 0. 1mm after comprehensive consideration.

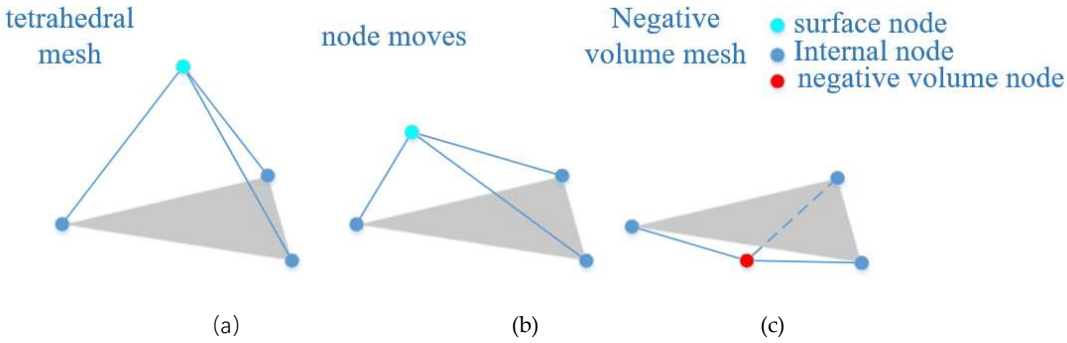

Fig. 4 Schematic Diagram of Node Displacement; (a) Tetrahedron element (b) node displacement element (c) element of negative volume

2. 4. Prediction of tool abrasion course and tool service

In order to predict tool abrasion course and tool service, the empirical formula of tool abrasion is hereby introduced, in which the finite element simulation results are put to work out the corresponding coefficient in formula. The metal cutting principle shows that there is complex exponential relation between abrasion loss VB of flank surface of tool and cutting parameter based on the confirmed machine tool characteristics and the geometrical parameter of tool, and the empirical formula of flank surface abrasion can be expressed in formula 6 :

$$VB = kv^{a1} f_z^{a2} a_p^{a3} a_e^{a4} t^{a5} \quad (6)$$

Wherein, VB represents the abrasion value of tool flank surface in simulation, and k represents abrasion coefficient of tool flank surface which is decided by work piece materials, tool materials and tool structure and refers to the abrasion influence index of tool flank surface, including the rotating

Preprints (www.preprints.org) | NOT PEER-REVIEWED | Posted: 4 November 2020 doi:10.20944/preprints202011.0189.v1

speed of main shaft, feed speed, axial cutting depth, radial cutting depth and cutting time. a_1、a_2、a_3、a_4、a_5 v、f_z、a_p、a_e、t take the logarithm on both sides in formula (6) to form linear function, namely

$$\begin{aligned} \lg VB = {} & \lg k + a1 \lg v^{a1} + a2 \lg f_z + a3 \lg a_p \\ & + a4 \lg a_e + a5 \lg t \end{aligned} \tag{7}$$

$y = \lg VB$、$a_0 = \lg k$、$x_1 = \lg v$、$x_2 = \lg f_z$、

Then $x_3 = \lg a_p$、$x_4 = \lg a_e$、$x_5 = \lg t$

$$y = a_0 + a_1 x_1 + a_2 x_2 + a_3 x_3 + a_4 x_4 + a_5 x_5 \tag{8}$$

Multiple linear regression equation is worked out as per formula 8:

$$\begin{cases} y_1 = A_0 + A_1 x_1 + A_2 x_2 + A_3 x_3 + A_4 x_4 + A_5 x_5 + \varepsilon_1 \\ y_2 = A_0 + A_1 x_6 + A_2 x_7 + A_3 x_8 + A_4 x_9 + A_5 x_{10} + \varepsilon_2 \\ \cdots\cdots\cdots \\ y_n = A_0 + A_1 x_{n+1} + A_2 x_{n+2} + A_3 x_{n+3} + A_4 x_{n+4} + A_5 x_{n+5} + \varepsilon_n \end{cases} \tag{9}$$

Wherein ε is the random error of simulation.

Formula (9) adopts matrix form and is expressed as:

$$Y = AX + \varepsilon \tag{10}$$

Wherein: $Y = \begin{Bmatrix} y_1 \\ y_2 \\ \cdots \\ y_n \end{Bmatrix}$ $A = \begin{Bmatrix} A_1 \\ A_2 \\ \cdots \\ A_5 \end{Bmatrix}$ $X = \begin{Bmatrix} 1 & x_{11} & x_{12} & x_{13} & x_{14} & x_{15} \\ 1 & x_{21} & x_{22} & x_{23} & x_{24} & x_{25} \\ 1 & \cdots & \cdots & \cdots & \cdots & \cdots \\ 1 & x_{n+1} & x_{n+2} & x_{n+3} & x_{n+4} & x_{n+5} \end{Bmatrix}$ $\varepsilon = \begin{Bmatrix} \varepsilon_1 \\ \varepsilon_2 \\ \cdots \\ \varepsilon_n \end{Bmatrix}$、、、

The least square method is adopted to evaluate parameters. A^* is evaluated with the least square method, with tropic equation as follows: a_1、a_2、a_3、a_4、a_5 A_1、A_2、A_3、A_4、A_5

$$\bar{y} = a_0 + a_1 x_1 + a_2 x_2 + a_3 x_3 + a_4 x_4 + a_5 x_5 \tag{11}$$

In the formula, $\bar{y}$ represents statistical variable and a_0、a_1、a_2、a_3、a_4、a_5 represents regression coefficient. Finally, the coefficient of the regression model is solved through Matlab programming and the time-varying curve of tool abrasion is shown in Fig. 5.

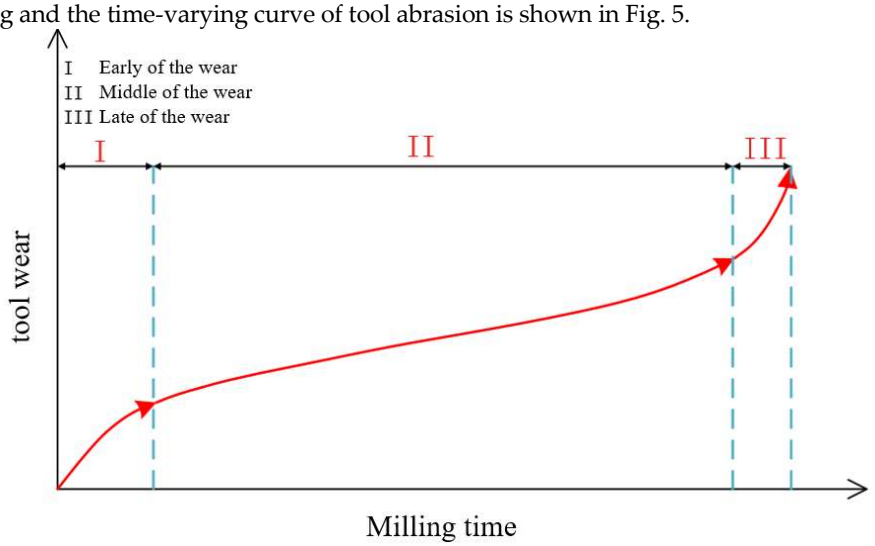

Fig. 5 Time-varying Curve of Tool Abrasion

3. Expression of different types of tool abrasion loss

Abrasion formula in subprogram is the core of the whole simulation program. Tool abrasion is a complex process due to coupling of several kinds of abrasion mechanism, and different abrasion mechanisms are mutually influenced. In the milling process, the tool mainly includes the following failure modes: tool abrasion, breakage, tipping, blade fracture, etc. The relationship between tool

Preprints (www.preprints.org) | NOT PEER-REVIEWED | Posted: 4 November 2020 doi:10.20944/preprints202011.0189.v1

abrasion mechanism and temperature is shown in Fig. 6[18] which shows close relationship between them. If temperature is low, the surface of tool mainly involves grains abrasion and adhesion abrasion. If the cutting temperature is high, the surface of tool mainly involves diffusion abrasion and oxidation abrasion.

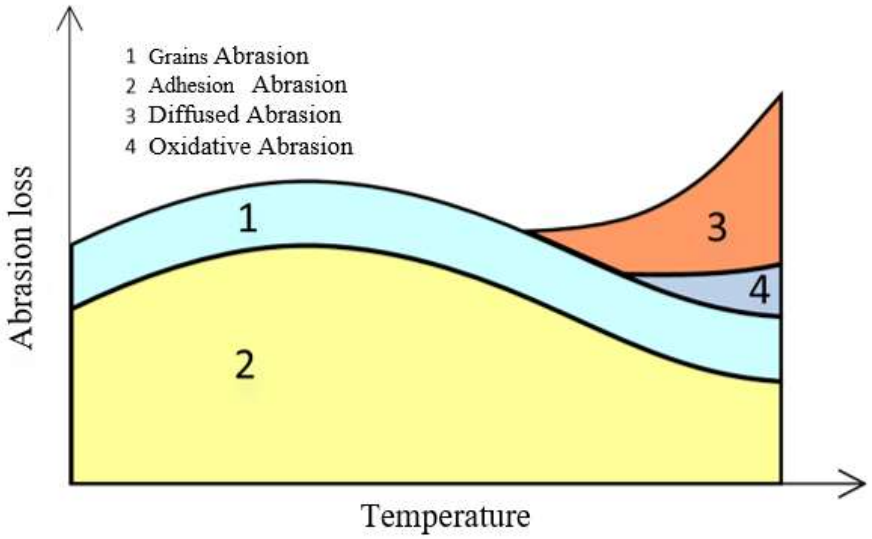

Fig. 6 Relationship between Tool Abrasion Mechanism and Temperature

3. 1. Adhesion abrasion (AD)

In the processing process of titanium alloy, tool abrasion is mainly divided into adhesion abrasion, grain abrasion and diffusion abrasion. Many scholars certify that, in high-speed cutting condition, the adhesion abrasion widely applied in actual scene for carbide cutter adopts the model proposed by usui et al. [19], as shown in formula 12.

$$\frac{W_n}{dt} = A_w \cdot \sigma_n \cdot v_c \exp(-B_w / (273+T)) \tag{12}$$

Wherein: W_n represents the adhesion abrasion loss, mm/min; A_w、B_w represents the abrasion constant obtained through experiment, which mainly depends on the tool materials and work piece materials. A_w、B_w indicates the titanium alloy cut with carbide cutter, its abrasion rate can be calculated through cutting experiment and its constant is calculated based on formula (1). σ_n represents the cutting stress on surface of tool, with unit of Mpa. v_c represents the sliding velocity of work piece materials, with unit of mm/min. T represents the cutting temperature, with unit of ℃. In milling of titanium alloy TC4, A_w and B_w are the experience value in general, in which the A_w is $7.8e^{-9}$ [17] and B_w is 2500[19]. So mathematical expression of final adhesion abrasion simulation is shown in formula 13:

$$\frac{W_n}{dt} = 7.8\times10^{-9} \cdot \sigma_n \cdot v_c \exp(-2500 / (273+T)) \tag{13}$$

3. 2. Grains abrasion (GA)

In cutting process, there are micro hard particles on contact surface between tool and work piece. With the relative movement between tool and cuttings, the groove is left on the surface of tool, namely tool has grains abrasion which is mainly related to the grains shape, hardness and distribution condition. In that case, Rainowicz et al. [19] researched grains abrasion and put forward the grains abrasion formula, as shown in formula 14:

Preprints (www.preprints.org) | NOT PEER-REVIEWED | Posted: 4 November 2020 doi:10.20944/preprints202011.0189.v1

$$\frac{W_a}{dt} = G \cdot v \tag{14}$$

Wherein, W_a represents grain abrasion, G represents grain abrasion constant, with unit of mm; V represents the relevant sliding velocity, with unit of mm/s. In milling of titanium alloy TC4, G[19] is $2.37e^{-11}$, so the final expression formula of grains abrasion is shown in formula 15:

$$\frac{W_a}{dt} = 2.37 \times 10^{-11} v \tag{15}$$

3. 3. Diffusion abrasion (DA)

In the milling and processing process, tool has low feed and high rotating speed in general. Under that condition, there is concentration difference and temperature difference in the elements in both tool and work piece, the elements in each part would rapidly diffuse, and the diffusion phenomenon concentrates on the contact area between abrasion belt of tool face and processing surface, as shown in Fig. 7.

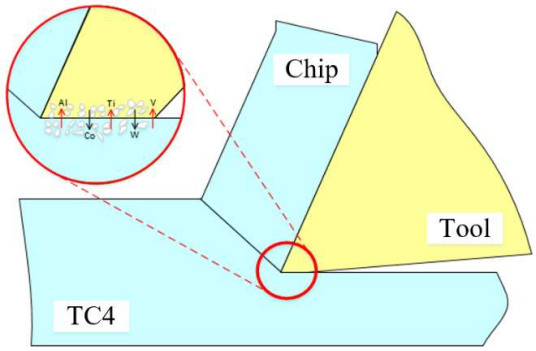

Fig. 7 Schematic Diagram of Diffusion Abrasion of Milling Cutter Flank Surface

For titanium alloy TC4, Sun Yujing of Shandong University [20] researched the carbide cutter abrasion, analyzed the influence of temperature on tool abrasion mechanism and established the tool abrasion model about temperature, with the diffusion abrasion formula of flank surface shown in formula 16:

$$\frac{W_r}{dt} = \frac{2C_0}{\rho}\left(\frac{vD_0}{x\pi}\right)^{\frac{1}{2}} e^{-Q/2R_Q(273+T)} \tag{16}$$

Wherein, W_a represents diffusion abrasion, C_0 represents the concentration of diffusion materials, D_0 represents equation coefficient, Q represents activation energy, ρ represents tool density, v represents relevant sliding velocity between flank surface and processed surface, x represents the distance between any point in tool-cuttings contact area and the cutting edge, RQ represents gas constant, and T represents temperature, with unit of °C. The above physical constants can be obtained based on relevant literature [20], as follows: $C_0 = 0.0253 mole/mm^3$, $D_0 = 1.9 mm^2/s$, $Q = 114.4 KJ/mole$, $R_Q = 8.315e-3 KJ/mole/K$ and $\rho = 14.9e3 kg/m^3$. Other data can be obtained through experiment or simulation, with the final expression formula as shown in formula 17:

$$\frac{W_r}{dt} = 3.3 \times \left(\frac{0.61v}{x}\right)^{\frac{1}{2}} e^{-6861/T} \tag{17}$$

Fig. 6 shows that there is mainly the grains abrasion and diffusion abrasion for interaction on the surface of tool when temperature is low, and the oxidation abrasion and diffusion abrasion occur when temperature is high. Based on that, Li Yousheng et al. [21], after experiment research, found that the element diffusion happens to cemented carbide and titanium alloy on the combination boundary when

Preprints (www.preprints.org) | NOT PEER-REVIEWED | Posted: 4 November 2020 doi:10.20944/preprints202011.0189.v1

the cutting temperature reaches 600 ℃. MATHEW et al. [22]researched and found the grains abrasion can be neglected when the cutting temperature exceeds 800℃. Based on the research of the above scholars, abrasion model can be divided into three stages based on temperature, as shown in formula 18:

$$\begin{cases} \dfrac{W}{dt}=\dfrac{W_n}{dt}+\dfrac{W_a}{dt}=7.8\times10^{-9}\cdot\sigma_n\cdot v_c\exp(-2500/(273+T)) \\ \qquad +2.37\times10^{-11}v \qquad (\mathrm{T}<600) \\ \dfrac{W}{dt}=\dfrac{W_n}{dt}+\dfrac{W_a}{dt}+\dfrac{W_r}{dt}=7.8\times10^{-9}\cdot\sigma_n\cdot v_c\exp(-2500/(273+T)) \\ \qquad +2.37\times10^{-11}v+3.3\times(\dfrac{0.61v}{x})^{\frac{1}{2}}e^{-6861/T} \qquad (600<\mathrm{T}<800) \\ \dfrac{W}{dt}=\dfrac{W_a}{dt}+\dfrac{W_r}{dt}=2.37\times10^{-11}v+3.3\times(\dfrac{0.61v}{x})^{\frac{1}{2}}e^{-6861/T} \qquad (\mathrm{T}>800) \end{cases} \tag{18}$$

In order to simulate the occurrence of diffusion abrasion of tool when temperature is over 600°C and the disappearing of diffusion abrasion when temperature is over 800°C, the temperature shall be controlled. The grains-adhesion abrasion is adopted in the area with temperature less than 600°C, grains-diffusion abrasion is adopted in the area with temperature between 600°C-800°C, and adhesion-diffusion abrasion is adopted in the area with temperature over 800°C. Schematic Diagram of Temperature Control is shown in Fig. 8.

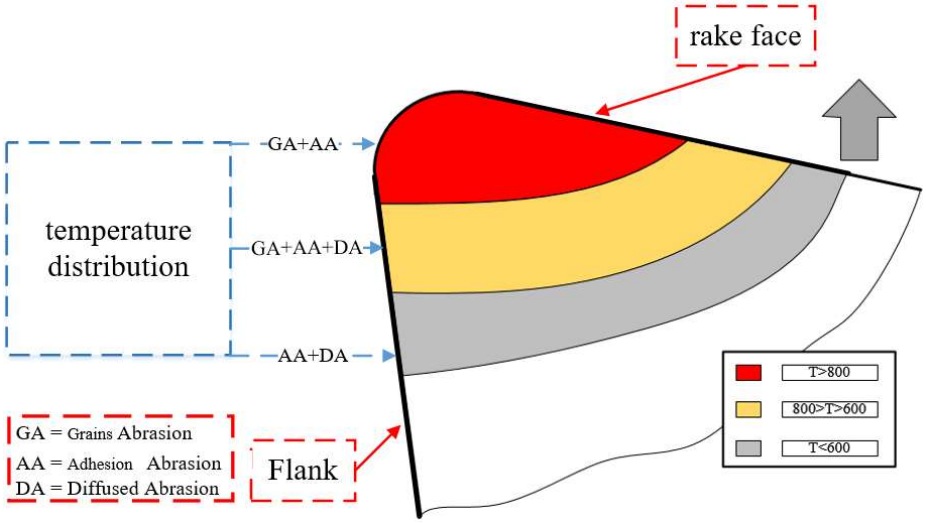

Fig. 8 Schematic Diagram of Tool Abrasion Type at Different Temperatures

4. Experimental verification and simulation results

4. 1. Milling experiment design

The processing experiment of milling is shown in Fig. 9 and is conducted on the VDL-100E triaxial numerically controlled machine tool produced by Dalian Machine Tool Group; The designed experiment works out the same parameters as simulation model, namely the cutting depth, milling width, feed speed and rotating speed of main shaft are 6mm, 3mm, 400mm/min and 2,000r/min, respectively. Since the influence of cutting fluid on tool abrasion isn't considered in model, the dry cutting is adopted in this experiment; The test adopts the cylindrical spiral blade end mill as tool, with the number of teeth, diameter, rake angle, clearance angle and helical angle of 2, 10mm, 8°, 9° and 55°, respectively; The test work piece adopts titanium alloy TC4, with dimension of 50*200*300mm. KEYENCE VHX- super-depth-of-field microscope is adopted to measure the tool abrasion loss of flank surface of milling cutter.

Preprints (www.preprints.org) | NOT PEER-REVIEWED | Posted: 4 November 2020 doi:10.20944/preprints202011.0189.v1

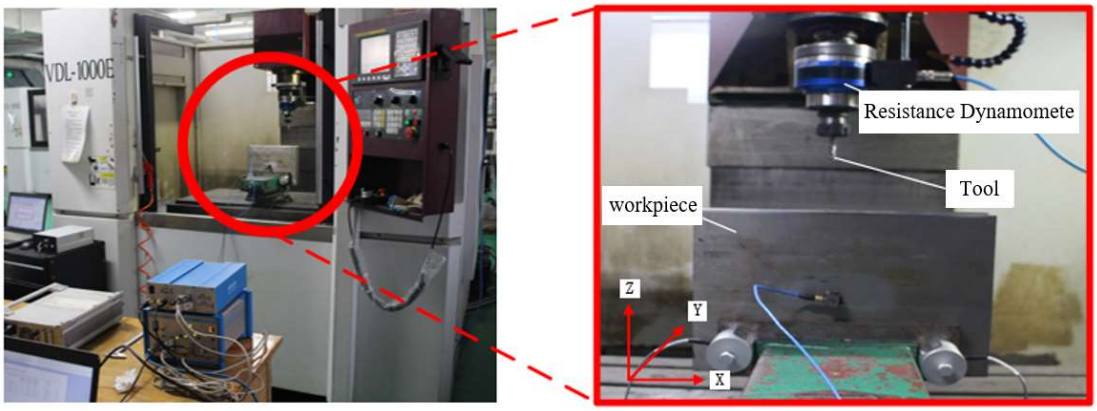

Fig. 9 Milling Processing Test Site

4. 2. Milling experimental results

In the experiment process, the abrasion characterization VB of tool flank surface is measured every eight minutes as per the experiment parameters, and the experiment measurement results are shown in 10. The figure shows that the tool abrasion mainly occurs on the flank surface of tool, and the abrasion depth increases with the increase of time. When tool abrasion reaches 113um, the quality of work piece surface decreases, which doesn't meet the processing requirements. Hence, the time when tool abrasion reaches 113um is deemed as the service life of tool.

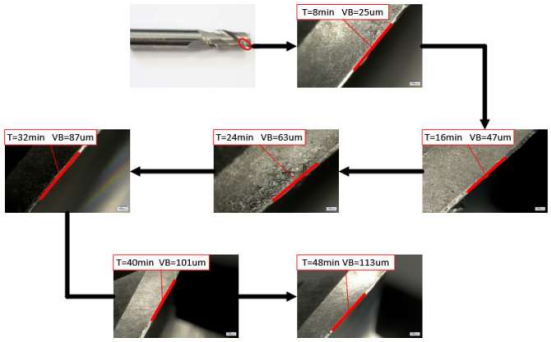

Fig. 10 Experimental Measurement Results

4. 3. Discussion of finite element simulation results

3. 3. 1 Analysis of temperature field results of tool

As shown in Fig. 11, Avg 75% in the picture means is default averaging threshold. when the first cutting edge of tool enters work piece, the temperature distribution results at cutting edge of tool show that the temperature doesn't rise sharply due to its hysteresis.

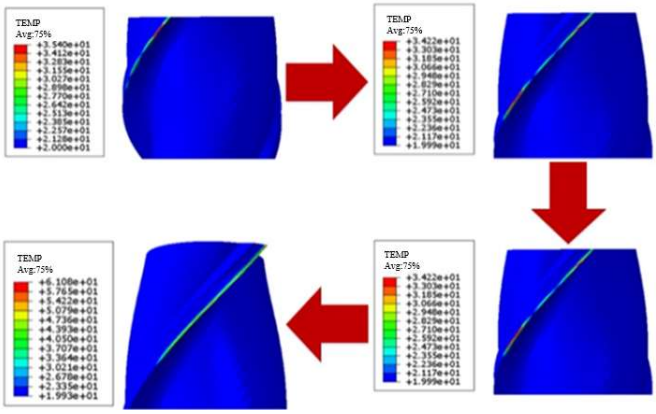

Fig. 11 Simulation Cloud Diagram for Cu**tting Edge into Workpiece**

Preprints (www.preprints.org) | NOT PEER-REVIEWED | Posted: 4 November 2020 doi:10.20944/preprints202011.0189.v1

When cutting is stable, as shown in Fig. 12, the temperature of tool cutting edge is about 500℃, but the temperature of tool nose is higher than that of cutting edge and reaches about 1,000℃, mainly because, in the continuous cutting process, there is extrusion-type cutting between tool nose and work piece at first, such cutting method would increase the friction effect between tool and work piece, then the heat concentrates on the tool nose and can't disperse easily in short time. While in other areas, temperature mainly shows the zonal distribution along the cutting edge, and temperature gradually decreases along the tool nose toward the shaft center direction of tool. So the tool nose wouldn't have severe abrasion in cutting process.

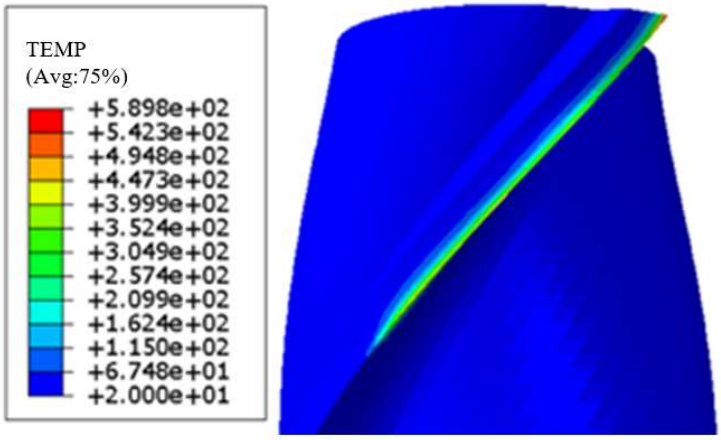

Fig. 12 Temperature of Cutting Edge after Stabilization

3. 3. 2 Analysis of tool abrasion results

Program is put in the simulation model through user subprogram to calculate the tool abrasion loss, as show in Fig. 13 which shows that the tool abrasion mainly happens at the cutting edge with zonal distribution. There is uneven abrasion at cutting edge, mainly due to larger contact stress at cutting edge in cutting process and accumulative abrasion as the increase of cutting times.

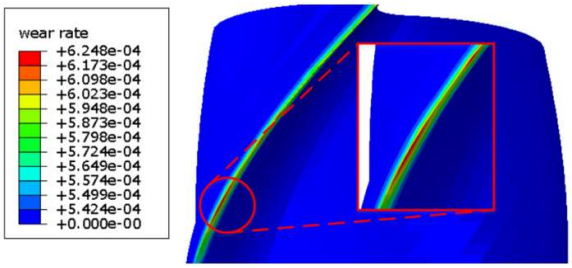

Fig. 13 Cloud Diagram of Tool Abrasion Loss (unit: mm/10s)

Based on the above method, the abrasion at different times is put in empirical formula to calculate constant, with calculation results shown in Table 3. The simulation results and experiment comparison of abrasion characterization VB for milling cutter flank surface are shown in Fig. 14.

Table 3 Parameters of Empirical Formula

k	a_1	a_2	a_3	a_4	a_5
0. 7573	-7. 277	3. 2676	9. 6475	8. 3551	0. 9567

The final expression formula is:

Preprints (www.preprints.org) | NOT PEER-REVIEWED | Posted: 4 November 2020 doi:10.20944/preprints202011.0189.v1

$$VB = 0.7573v^{-7.2776} f_z^{3.2676} a_p^{9.6475} a_e^{8.3551} t^{0.9567}$$

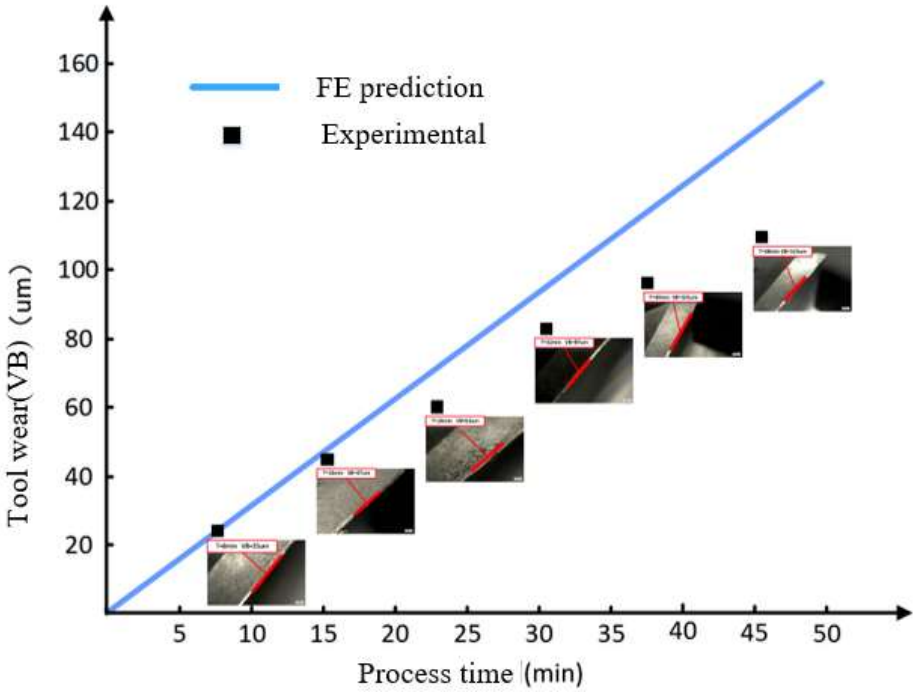

Fig. 14 Comparison of Abrasion VB between Simulation and Experiment for Milling Cutter Flank Surface

Fig. 14 shows that the experiment results of end mill flank surface abrasion VB keep consistent with change trend, which verifies the feasibility of such method. Fig. 14 shows that the predicted value is larger than the actual measured value, mainly because the predicted simulation abrasion mainly refers to preliminary abrasion which is relatively fierce, without stable periods of medium-term abrasion. The error of this method is within 30%, mainly due to the following factors:

1. Error caused by grid dimension: The grid dimension decides the simulation precision. Oversized grid is difficult to guarantee the simulation precision and undersized grid causes too long simulation time. Hence, the appropriate grid dimension shall be selected after comprehensive consideration.

2. Milling vibration factors aren't considered in the established simulation process of finite element simulation model.

3. The tool abrasion caused due to tipping isn't considered in simulation process, and the tool Mises press is mainly observed to find tool tripping in the finite element simulation.

4. In the milling process of cemented carbide end mill, there is oxidation abrasion on its flank surface, but the oxidation abrasion isn't considered in the abrasion prediction model.

5. Conclusions

The simulation model of tool abrasion and the prediction model of tool service life based on finite element simulation method are established on account of the cutting processing process of Ti6Al4V to work out the distribution condition of tool nose temperature and contact stress and accurately predict the abrasion condition of tool flank surface. The research results provide reasonable technical support for monitoring tool abrasion status, predicting tool service life and optimizing tool structure. The conclusion is as follows:

1. On account of the change of tool abrasion type at different temperatures, the carbide cutter abrasion model considering temperature effect is constructed to avoid the limitation of single model and improve the prediction precision of tool abrasion;

2. Combined the simulation results with the empirical formula， the tool abrasion course function can be calculated, which saves lots of simulation time and realizes the rapid prediction of tool service life;

3. The test about on the service life of tool is carried out, and the simulation results and experiment measurement results are compared and analyzed. The simulation results can simulate the change rules of tool abrasion in cutting process better, and prediction error is within 30%, which can predict service life of tool to some extent.

Funding: This research was funded by National Natural Science Foundation of China, grant number：5171001055，National key RESEARCH and development programs，grant number：2019YFB1704800.

Acknowledgments: Thanks are due to Chen Zhitao for assistance with the experiments .

Conflicts of Interest: The authors declare no conflict of interest.

References

1. S. K , Choudhury, and, et al. Tool wear prediction in turning[J]. Journal of Materials Processing Technology, 2004,153-154:276-280.
2. Zhou J M , Walter H , Andersson M , et al. Effect of chamfer angle on wear of PCBN cutting tool[J]. International Journal of Machine Tools & Manufacture, 2003, 43(3):301-305.
3. Denkena B , Lucas A , Bassett E . Effects of the cutting edge microgeometry on tool wear and its thermo-mechanical load[J]. CIRP Annals - Manufacturing Technology, 2011, 60(1):73-76.
4. Rathod K B , Lalwani D I . Modeling of flank wear progression for coated cubic boron nitride tool during hard turning of AISI H11steel[J]. Materials Today: Proceedings, 2018, 5(2):6692-6701.
5. H. Z. Liu, Wenjun Zong. Prediction model of tool wear volume in precision turning of ceramic particle reinforced aluminum matrix composites[J]. The International Journal of Advanced Manufacturing Technology（Int J Adv Manuf Technol）, 2019, 100(9-12)：2689-270
6. Guicai Zhang, Changsheng Guo. Modeling Flank Wear Progression Based on Cutting Force and Energy Prediction in Turning Process[J]. Procedia Manufacturing, 2016, 5：536-545.
7. Salman Pervaiz, Ibrahim Deiab, Amir Rashid, Mihai Nicolescu. Minimal quantity cooling lubrication in turning of Ti6Al4V: Influence on surface roughness, cutting force and tool wear[J]. Proceedings of the Institution of Mechanical Engineers, Part B: Journal of Engineering Manufacture(Proc IMechE Part B:J Engineering Manufacture), 2017, 231(9)：1542-1558.
8. P. C. Wanigarathne, A. D. Kardekar, O. W. Dillon, G. Poulachon, I. S. Jawahir. Progressive tool-wear in machining with coated grooved tools and its correlation with cutting temperature[J]. Wear, 2005, 259(7-12)：1215-1224.
9. A. Attanasio,E. Ceretti. 3D finite element analysis of tool wear in machining[J]. Manfacturing Technology,2008, 57:61-64.
10. M. Binder,F. Klocke. An advanced numerical approach on tool wear simulation for tool and process design in metal cutting[J]. Simulation Modelling Practice and Theory,2017,70: 65-82.
11. Mohammad Lotfi. 3D FEM simulation of tool wear in ultrasonic assisted rotary turning[J]. Ultrasonics,2018,88: 106-114.
12. Attanasio A , Faini F , Outeiro J C . FEM Simulation of Tool Wear in Drilling[J]. Procedia CIRP, 2017, 58:440-444.
13. Xie L J , Schmidt J , Schmidt C , et al. 2D FEM estimate of tool wear in turning operation[J]. Wear, 2005, 258(10):1479-1490.
14. SUN Yujing,SUN Jie,LI Jianfeng. Finite Element Analysis on Prediction of Tool Wear in Milling Titanium[J]. Journal of Mechanical Engineering, 2016, v. 52(05):199-207.
15. Malakizadi A , Gruber H , Sadik I , et al. An FEM-based approach for tool wear estimation in machining[J]. Wear, 2016:S004316481630182X.

16. YUE Caixu，LIU Xin et. al. Tool optimization for stitching die milling based on finite element simulation[J]. Chinese Journal of Mechanical Engineering, 2019, v. 52(05):199-207.
17. Wang Xiaoqin, Study on Tribologieal Behaviorand Tool Life in Ti6A14V High Performance Maehining[D]. Shandong University,2009.
18. Li Kailing,Song Qiang, Fundamentals of Mechanical Manufacturing Technology[M]. Jinan: Shandong science and technology press. 2008.
19. USUI E，SHIRAKASHI T，KITAGAWA T. Analytical prediction of cutting tool wear[J]. Wear，1984，100(1)：129-151.
20. SUN Yujing . Parametric Modeling of Milling Titanium Alloy and Prediction of Tool Wear State[D]. Shandong University
21. Li Yousheng. Chemieal Performance match between cemented Carbide tools and Ti-6Al-4V alloy[D]. Shandong University. 2010.
22. MOLINARI A，NOUARI M. Modeling of tool wear by diffusion in metal cutting[J]. Wear,2002，252：135-149.